FORWARD-IN-TIME DIFFERENCING FOR FLUIDS

Piotr K. Smolarkiewicz
National Center for Atmospheric Research[1]
Boulder, Colorado 80307 USA

Summary: This paper discusses the extension of the dissipative advection schemes, often referred to in meteorological literature as Crowley-type schemes, on advection equations with arbitrary forcing and/or source terms included. Since such equations constitute a prototype of evolution equations for fluids, the considerations herein are relevant to a variety of atmospheric applications. The thesis of this paper is that no matter how accurate the advection scheme employed, the entire evolution equation is approximated to, at most, $\mathcal{O}(\Delta t)$, which is a consequence of disregarding forcing terms in the derivation of Crowley-type schemes. The consequences of this truncation error may be quite severe depending upon the particular problem at hand. The remedy discussed is simple and easy to implement in any numerical model using forward-in-time differencing. Theoretical considerations are illustrated with idealized tests and simple examples of flows of density stratified fluid past two-dimensional mountains.

1. INTRODUCTION

Prognostic equations for fluids may be written in a compact form

$$\frac{\partial \psi^\beta}{\partial t} + \nabla \circ (\mathbf{v}\psi^\beta) = R^\beta(\boldsymbol{\psi}), \quad {}_{\beta=1,\ldots,N} \ , \tag{1}$$

where $\boldsymbol{\psi} \equiv (\psi^1, ..., \psi^N)$ is a vector of N variables describing the state of the fluid, $\mathbf{v}$ is the velocity vector, and R^β combines all forcings and/or sources. Although in many applications $\mathbf{v}$ is identical with, say, (ψ^1, ψ^2, ψ^3), in general, $\mathbf{v}$ is a function of the fluid variables. Finite-difference discretization of (1) fall into two conceptually distinct categories. In the first category, all terms in (1) are independently approximated to a desired order of accuracy; this leads, for instance, to a class of centered-in-time-and-space algorithms. The elementary example of such a discretization is a popular, second-order-accurate leap-frog scheme, which for the evolution of a fluid variable $\psi^\beta = \phi(x,t)$ in one spatial dimension takes the simple form

$$\frac{\phi_i^{n+1} - \phi_i^{n-1}}{2\Delta t} + \frac{(u\phi)_{i+1}^n - (u\phi)_{i-1}^n}{2\Delta X} = R_i^n(\phi) \ , \tag{2}$$

[1] The National Center for Atmospheric Research is sponsored by the National Science Foundation

where n and i have their usual meaning of a temporal and spatial position on a discrete, regular grid with the temporal and spatial increments Δt and ΔX, respectively.

In the second category of discretization, the temporal derivatives in (1) are approximated with forward-in-time differences; and the truncation errors proportional to temporal derivatives of ψ^β are appropriately compensated by exploiting information contained in system (1). This approach leads to a class of Lax-Wendroff approximations [see Section 12.7 in Richtmyer and Morton (1967), and Section 5.E.5 in Roache (1972) for discussions]. The elementary example of such an approximation is the second-order-accurate transport algorithm, often referred to as the Crowley (1968), or Leith (1965), advection scheme. For a constant one-dimensional flow U and vanishing forcings, the Lax-Wendroff algorithm may be written as

$$\frac{\phi_i^{n+1} - \phi_i^n}{\Delta t} + U\frac{\phi_{i+1}^n - \phi_{i-1}^n}{2\Delta X} - \frac{1}{2}U^2\Delta t\frac{\phi_{i+1}^n - 2\phi_i^n + \phi_{i-1}^n}{\Delta X^2} = 0\ , \tag{3}$$

wherein the last term on the l.h.s of (3) compensates the first-order truncation error $\frac{1}{2}\Delta t\frac{\partial^2\phi}{\partial t^2}$ inherent in the forward-in-time discretization of (1). As the complete Lax-Wendroff algorithms for fluids were designed to deal with the conservation laws

$$\frac{\partial\psi}{\partial t} + \nabla \circ [\mathbf{F}(\psi)] = 0\ , \tag{4}$$

they are not particularly attractive for atmospheric applications where Coriolis forces, phase-change processes, coordinate transformations, and various microphysical or chemical sinks and sources cause departures of governing equations from the conservation-law form. This and the considerable complexity of the Lax-Wendroff schemes[2] are perhaps responsible for their marginal popularity in the atmospheric community. Nonetheless, the leading philosophy of the Lax-Wendroff approach shines through many approximations to atmospheric problems.

In the absence of forcings, system (1) reduces to a decoupled set of the advection transport equations, which may be approximated separately using an advection algorithm of desired properties. The literature on advection schemes is enormous (see

[2] See Houghton and Kasahara (1968) for an example of the Lax-Wendroff approximation to shallow water equations.

Rood, 1987, for a recent review). Among a variety of approaches, the forward-in-time schemes (sometimes referred to for brevity as dissipative schemes) have a long tradition in the meteorological literature. The elementary approximations of Leith (1965), Crowley (1968), and Tremback et al. (1987), as well as more specialized approaches of Smolarkiewicz (1983), Takacs (1985), and Bott (1989), may all be viewed as derivatives of a general Lax-Wendroff concept regardless of their diverse means of derivation.[3] Under certain circumstances all these algorithms may be reduced to either the simple scheme in (3) or some slight modification of (3). The dissipative advection schemes have important advantages: They offer arbitrary accuracy for uniform flows (Tremback et al., 1987), do not contain computational modes, require less storage than multiple-time-level algorithms, and are easy to modify and code. In order to implement such approximations for the evaluation of a general system (1), however, several difficulties must be overcome.

The elementary dissipative advection schemes were customarily derived for uniform one-dimensional flows. Their extension to multidimensional problems is often resolved by means of the alternate-direction (time-split) approach. However, in order to maintain the second-order accuracy of the time-split solutions one must ensure that the scheme employed in every alternation is fully second-order-accurate (Strang, 1968). This requirement is not necessarily satisfied by elementary advection schemes whose leading $\mathcal{O}(\Delta t)$ truncation error depends on the partial (temporal and spatial) derivatives of the advecting velocity (Crowley, 1968); this deficiency of the elementary schemes may lead to weak instabilities in essentially inhomogeneous flows (Petschek and Libersky, 1975; Smolarkiewicz, 1982). In incompressible, steady flows, the second-order-accurate dissipative approximations are achieved by employing the philosophy of the Lax-Wendroff approach directly to a multidimensional advection problem (Dukowicz and Ramshaw, 1979; Smolarkiewicz, 1982, 1984; Gresho et al., 1984). These concepts may be further extended onto compressible (Smolarkiewicz, 1984) and time-dependent flow fields (Smolarkiewicz, 1985; Smolarkiewicz and Clark, 1986).

Providing dissipative transport algorithms capable of approximating an arbitrary advection problem to at least second-order accuracy, one might anticipate that adequate approximation to the general system (1) easily follows. A common approach, which

[3] See Bleck (1984a) for a discussion of various derivations of the Lax-Wendroff scheme.

draws from the first category of approximations [recall the discussion following (1)], is to apply a suitable dissipative advection scheme to the l.h.s of (1) and to approximate the r.h.s of (1) to a desired order of accuracy. Unfortunately (as will be shown in the following section), such an approximation is only $\mathcal{O}(\Delta t)$ accurate, which is a consequence of disregarding forcing/source terms in the derivation of the dissipative advection schemes. Thus, the second-order-accurate, forward-in-time integration of (1) requires more effort than a direct application of a second-order-accurate dissipative advection scheme.

The next section derives the explicit form of the first-order truncation error terms due to the forward-in-time discretization of (1), and discusses their consequences and means of compensation. Section 3 illustrates the theoretical considerations with idealized tests and examples of applications to a problem of density stratified fluid flow past a two-dimensional mountain.

2. SECOND-ORDER DISSIPATIVE DIFFERENCING OF EQ. (1)

In order to design a second-order dissipative approximation to (1), it is convenient to consider a single equation

$$\frac{\partial \phi}{\partial t} + \nabla \circ (\mathbf{v}\phi) = R \, . \tag{5}$$

The temporal discretization of (5) is assumed as

$$\frac{\phi^{n+1} - \phi^n}{\Delta t} + \nabla \circ (\mathbf{v}^{n+1/2}\phi^n) = R^{n+1/2} \, . \tag{6}$$

Although the discretization in (6) contains certain elements of time-centering, it is essentially forward-in-time insofar as the advective transport of ϕ is concerned.[4] Expanding (6) into the second-order Taylor sum about $t = n\Delta t$ gives

$$\frac{\partial \phi}{\partial t} + \frac{1}{2}\Delta t \frac{\partial^2 \phi}{\partial t^2} + \nabla \circ \left[(\mathbf{v} + \frac{1}{2}\Delta t \frac{\partial \mathbf{v}}{\partial t})\phi\right] = R + \frac{1}{2}\Delta t \frac{\partial R}{\partial t} + \mathcal{O}(\Delta t^2) \, , \tag{7}$$

[4] Taking $\mathbf{v}$ and R at $n+1/2$ time-level in (6) will lead to cancellation of the truncation error terms that depend on temporal derivatives of the advecting velocity and forcing; in applications, such a temporal staggering may be achieved by means of either interpolation or extrapolation, depending upon the particular problem at hand (see Section 3 for examples).

which is the continuous equation implied by the discretization in (6), i.e., ϕ approximated by (6) satisfies (7) rather than (5) (see Warming and Hyett, 1974, for discussion). Taking $\frac{\partial}{\partial t}(7)$ results in

$$\frac{\partial^2\phi}{\partial t^2} + \nabla \circ (\frac{\partial \mathbf{v}}{\partial t}\phi + \mathbf{v}\frac{\partial \phi}{\partial t}) = \frac{\partial R}{\partial t} + \mathcal{O}(\Delta t) \; . \tag{8}$$

Since (7) implies

$$\frac{\partial \phi}{\partial t} = -\nabla \circ (\mathbf{v}\phi) + R + \mathcal{O}(\Delta t) \; , \tag{9}$$

(8) may be rewritten as

$$\frac{\partial^2\phi}{\partial t^2} = \nabla \circ \big[-\frac{\partial \mathbf{v}}{\partial t}\phi + \mathbf{v}(\mathbf{v} \circ \nabla\phi) + \mathbf{v}\phi(\nabla \circ \mathbf{v}) - \mathbf{v}R\big] + \frac{\partial R}{\partial t} + \mathcal{O}(\Delta t) \; . \tag{10}$$

Equation (10) evaluates $\frac{\partial^2\phi}{\partial t^2}$ by exploiting (7), or equivalently (9), which are viewed as continuous equations solved exactly by the algorithm in (6). Relationships similar to (10) were sometimes derived in the literature for problems with vanishing forcings by taking $\frac{\partial}{\partial t}(5)$ and reusing (5) instead of (9). Insofar as the second-order-accurate schemes are concerned, both procedures are equivalent; a rigorous exploitation of (7) instead of (5) becomes essential while designing higher-order-accurate methods.

Implementation of (10) in (7), and regrouping the terms that do not cancel, leads finally to

$$\frac{\partial \phi}{\partial t} + \nabla \circ (\mathbf{v}\phi) = R - \nabla \circ \big[\frac{1}{2}\Delta t \mathbf{v}(\mathbf{v} \circ \nabla\phi) + \frac{1}{2}\Delta t \mathbf{v}\phi(\nabla \circ \mathbf{v})\big] + \nabla \circ (\frac{1}{2}\Delta t \mathbf{v}R) + \mathcal{O}(\Delta t^2), \tag{11}$$

wherein all $\mathcal{O}(\Delta t)$ errors due to the forward-in-time differencing in (6) are already expressed by spatial derivatives. Consequently, an $\mathcal{O}(\Delta t^2)$ scheme for (5) may be achieved by subtracting from the r.h.s of (6) forward-in-time approximations (or backward-in-time approximations, whichever is more convenient in an application) of the remaining truncation error terms.

The forcing-independent truncation error terms in (11), as well as their consequences and means of compensation, are already familiar: In a simple one-dimensional case of a uniform flow U with $R \equiv 0$ in (5), the only remaining error term in (11) is $-\frac{\Delta t}{2}U^2\frac{\partial^2\phi}{\partial x^2}$; assuming centered-in-space discretization and subtracting this term

from the r.h.s of (6) results in the classic Lax-Wendroff advection scheme (3). The extensions on multidimensional incompressible flows ($\nabla \circ \mathbf{v} = 0$) were discussed in Dukowicz and Ramshaw (1979), Smolarkiewicz (1982), and Gresho et al. (1984),[5] whereas compensation of the errors $\sim \nabla \circ \mathbf{v}$ has been addressed in Smolarkiewicz (1984). The remaining, forcing-dependent, first-order error term $\frac{1}{2}\Delta t \nabla \circ (\mathbf{v}R)$, to the author's knowledge, has thus far eluded attention. Consequences of this error may be quite serious. In order to acquire some insight, consider an incompressible flow in (5) and a fully second-order advection scheme for spatial discretization in (6). The continuous "energy" equation implied by the discretization is then

$$\frac{\partial \phi^2}{\partial t} + \mathbf{v} \circ \nabla \phi^2 = 2\phi R + \Delta t \phi \mathbf{v} \circ \nabla R + \mathcal{O}(\Delta t^2) \; . \tag{12}$$

The first-order error term on the r.h.s of (12) has the sense of a spurious source or sink of ϕ^2; in any case, it may be destructive for the stability of computations (an excessive sink can lead to negative "energy" and imaginary solutions).

The compensation of the $\frac{1}{2}\Delta t \nabla \circ (\mathbf{v}R)$ error in (11) may be achieved in many ways depending upon the particular problem of interest and spatial discretization employed. A simple and efficient manner is to subtract from the r.h.s of (6) the donor cell (alias upwind, upstream) approximation to the error term. The resulting second-order-accurate dissipative algorithm for (5) can then be compactly written as

$$\phi_{\mathbf{i}}^{n+1} = \phi_{\mathbf{i}}^{n} - \mathcal{AI}_{\mathbf{i}}(\phi^n, \boldsymbol{\alpha}^{n+1/2}) + R_{\mathbf{i}}^{n+1/2}\Delta t - \mathcal{A}_{\mathbf{i}}(\frac{\Delta t}{2} R^n, \boldsymbol{\alpha}^n) \; , \tag{13}$$

where $\mathcal{AI}$ is an advective-flux-divergence operator from a selected (at least second-order-accurate) dissipative advection scheme, $\mathcal{A}$ is the same operator but from the first-order-accurate donor cell scheme, $\boldsymbol{\alpha}$ is a vector of local Courant numbers, and $\mathbf{i}$ denotes the position on a grid. The choice of the donor cell approximation for compensation of the error term is not accidental; it follows a general guideline that maintaining the dissipativeness of the entire approximations one order higher than that of the approximation benefits computational stability (see Section 5.4 in Richtmyer and

[5] Note this important aspect: even if a fully multidimensional advection scheme achieves second-order accuracy, its alternate-direction (time-split) counterpart does not, since $\nabla \circ \mathbf{v} \neq 0$ in alternations.

Morton, 1967). Conversely, choosing a centered-in-space approximation to the error term might destabilize the solution: Consider, for instance,

$$R_{\mathrm{i}}^{n+1/2} = \frac{1}{2}(R_{\mathrm{i}}^{n+1} + R_{\mathrm{i}}^{n}) \tag{14}$$

for approximation of the time-centered forcing term in (11), and note that the last two terms of the resulting algorithm

$$\phi_{\mathrm{i}}^{n+1} = \phi_{\mathrm{i}}^{n} - \mathcal{AI}_{\mathrm{i}}(\phi^{n}, \alpha^{n+1/2}) + \frac{\Delta t}{2} R_{\mathrm{i}}^{n+1} + \frac{\Delta t}{2} R_{\mathrm{i}}^{n} - \mathcal{AI}_{\mathrm{i}}(\frac{\Delta t}{2} R^{n}, \alpha^{n}) \tag{15}$$

combine into the donor cell advection of $\frac{\Delta t}{2} R$, which is stable for appropriately bounded α. Choosing instead the centered-in-space approximation would result in an unconditionally unstable Euler advection scheme.

Equation (15) exposes another important aspect of the approximation adopted. Rewriting (15) as

$$\phi_{\mathrm{i}}^{n+1} = \phi_{\mathrm{i}}^{n} - \mathcal{AI}_{\mathrm{i}}(\phi^{n}, \alpha^{n+1/2}) + \frac{\Delta t}{2} R_{\mathrm{i}}^{n+1} + \frac{\Delta t}{2}(R_{\mathrm{i}}^{n} - \mathcal{AI}_{\mathrm{i}}(R^{n}, \alpha^{n})) \tag{16}$$

and assuming an incompressible flow in (5),[6] one can observe easily that the last expression on the r.h.s of (16) represents the product of $\frac{\Delta t}{2}$ and the first-order-accurate approximation to the forcing evaluated at the departure point of the trajectory arriving at the grid point $(\mathrm{i}, n+1)$. Consequently, the last three terms on the r.h.s of (15) combine into the second-order-accurate trapezoidal-rule integral of forces along a parcel trajectory. Since the first two terms on the r.h.s of (15) approximate ϕ at the departure point, the algorithm in (15) approximates with second-order accuracy the Eulerian evolution equation (5) as well as its Lagrangian counterpart

$$\frac{d\phi}{dt} = R\,. \tag{17}$$

[6] Although the arguments herein rely heavily on the incompressibility assumption, a more elaborated discussion employing the mass continuity equation would lead to a similar conclusion with ϕ and R replaced in (17), respectively, by $\phi\rho^{-1}$ and $R\rho^{-1}$, where ρ is a fluid density.

3. COMPUTATIONAL EXAMPLES

3.1 Solid body rotation test with a linear source

In order to illustrate the theoretical considerations of the preceding section, we consider first the traditional problem of a rotating cone; such a test has often been used to document properties of advection schemes (see, for example, Smolarkiewicz, 1982, 1984). For the sake of simplicity we assume $R = -\frac{1}{\tau}\phi$ in (5). Such a source function may be viewed as a prototype of a linear chemical reaction. The characteristic time scale of the source is assumed to be $\tau = 10^{-2}T$, where T is the revolution period. The radius of the cone's base is equal to 15 grid intervals of the uniform mesh consisting of 101×101 grid points; and the initial height of the cone is $H\exp(100)$, where H is the true height of the cone after one revolution. The analytic solution after one revolution of the cone is shown in Fig. 1a; the reference spikes in the upper right and lower left corners are equal to H and $0.5H$, respectively. Figure 1b shows the corresponding numerical solution (628 time steps with the maximum Courant number equal to unity) obtained with (13), where the $\mathcal{ATT}$ operator employs the basic, second-order-accurate, multidimensional, positive definite advection transport algorithm (MPDATA) of Smolarkiewicz (1984), and $R^{n+1/2}$ is approximated with the trapezoidal (implicit) rule (14). Figure 1c shows a similar solution in which compensation of the source-dependent error term has been disregarded. Comparing the two figures clearly shows that the error due to coupling the advection with sources is noticeable — its neglect results in an underestimated amplitude and a phase shift of the solution.

The simple example employed demonstrates that compensation of the forcing-dependent truncation error improves accuracy of integrations. However, since in the current test the rate of decay is about 0.85 per time step, it is not clear whether observed accuracy improvements are of any practical importance, and whether they are worth the effort. In order to clarify this issue, we consider below a simple dynamic example that admits nonlinear coupling of fluid variables.

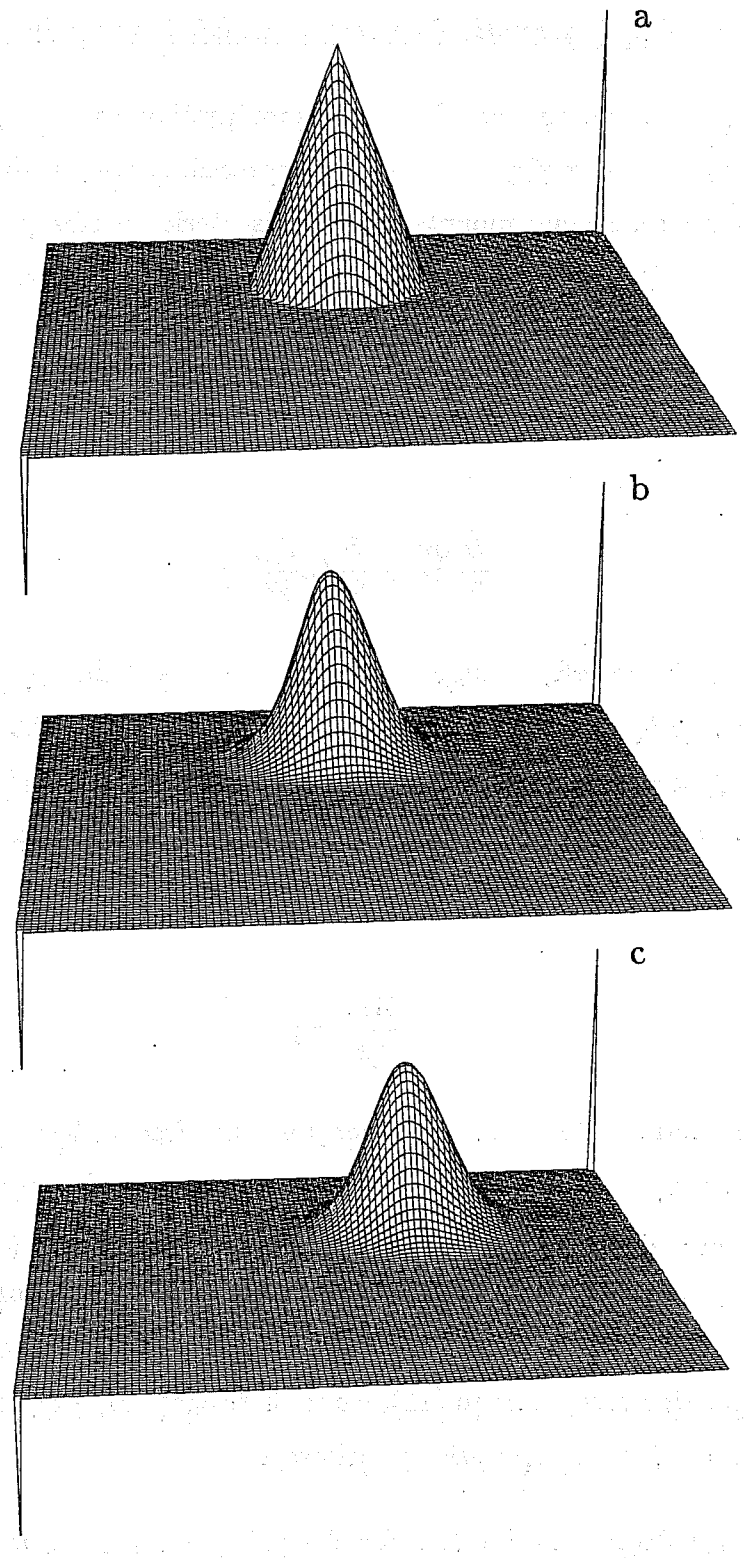

Figure 1. The decaying, rotating cone test. The analytic (plate **a**) and the two different numerical solutions are all shown after one revolution of the cone. The reference spikes in the upper-right and the lower-left corners represent the true- and minus-half-of-the-true-height of the cone. Plate **b** shows the second-order-accurate, sign-preserving dissipative solution which takes into account truncation errors due to coupling between advection and sources, whereas plate **c** shows a similar solution which disregards the coupling errors.

3.2 Density stratified, hydrostatic flow past an isolated mountain in isosteric coordinates

In the current example we consider an approximation to the system of equations governing hydrostatic flow of an inviscid, incompressible, nonrotating, density stratified fluid past a two-dimensional mountain in the isosteric coordinates (cf. Smith, 1989; Bleck and Smith, 1990). The system (1) takes then a simple form

$$\frac{\partial m}{\partial t} + \frac{\partial}{\partial x}(um) = -\frac{\partial p}{\partial s}\frac{\partial M}{\partial x} \ , \tag{18a}$$

$$\frac{\partial}{\partial t}\frac{\partial p}{\partial s} + \frac{\partial}{\partial x}(u\frac{\partial p}{\partial s}) = 0 \ , \tag{18b}$$

where $s \equiv \rho^{-1}$ is the specific-volume, vertical coordinate of the model, p is the pressure, $m \equiv u\frac{\partial p}{\partial s}$ is the horizontal momentum, and $M \equiv gh + sp$ is the Montgomery potential with h and g denoting the actual height of a density surface and the acceleration of gravity, respectively. The prognostic equations for momentum and mass continuity are supplied with the diagnostic relationship of the hydrostatic balance of the fluid

$$\frac{\partial M}{\partial s} = p \ . \tag{19}$$

The upper boundary condition incorporates the free-surface assumption, $(p = \text{const})_s \rightarrow \infty$, whereas for the lower boundary a material surface is assumed. Note that due to the specific choice of the vertical coordinate the resulting momentum equation departs from the conservation-law form (4) characteristic of the Euler equations. Since a goal of this section is to emphasize the importance of compensating the forcing-dependent truncation error term in (11), we shall discuss only briefly other physical and numerical aspects of the computations performed.

There are several degrees of freedom for designing a second-order approximation to a system consisting of (18) and (19), and many different discretizations may be considered. Herein, we select one that is convenient for the problem at hand. In the horizontal, all variables are defined at the same grid-point positions; in the s-direction, the pressure is staggered with respect to all other variables. The temporal discretization follows (13), where $\mathcal{ATT}$ employs the nonlinear MPDATA scheme whose

design, properties, performance, and various options were documented in a series of publications (Smolarkiewicz, 1983, 1984; Smolarkiewicz and Clark, 1986; Margolin and Smolarkiewicz, 1989; Smolarkiewicz and Grabowski, 1990). The general concept of the algorithm is that of the dissipative advection schemes; however, compensation of the leading truncation error terms is nonlinear. It is achieved through the iterative application of the donor-cell scheme where the second and following iterations use pseudo velocity fields, obtained from renormalization of the truncation errors of the donor-cell scheme into the form of donor-cell fluxes. The MPDATA family of algorithms offers a variety of options of different accuracy, computational efficiency, and complexity levels. The version of MPDATA selected in the current example compensates the entire, forcing-independent error term on the r.h.s of (11) and preserves the signs of the transported variables. The sign-preservation property of the scheme is essential: it prevents development of spurious negative pressure thicknesses of isosteric layers (which could lead to "convective" instability) and bounds the total "energy" of the scheme, necessary for the nonlinear stability of the system (For discussion, see the accompanying paper in this volume). The MPDATA schemes assume flux form and require the advective Courant numbers to be staggered-in-space with respect to a transported variable. This spatial staggering is achieved by averaging the velocity variable between the two adjacent grid points, whereas the temporal staggering, assumed in (6) and (13), employs extrapolation of the velocities from $n-1$ and n temporal levels (see Smolarkiewicz and Clark, 1986, for discussion). In order to prevent spurious accelerations due to pressure forces from zero-thickness layers (the issue discussed in detail by Bleck, 1987, and Bleck and Smith, 1990) the horizontal derivative of the Montgomery potential is approximated with the second-order-accurate pressure-thickness-weighted average of the one-sided derivatives; in essence, such an approximation follows that of Bleck and Smith (1990). In order to simulate an infinite extent of the fluid, a gravity-wave absorber (Klemp and Lilly, 1978) is employed in the upper portion of the model; and the Davies (1983) relaxation scheme is incorporated at the lateral boundaries of the computational domain.

The time-step advancement of the discrete equations proceeds in three stages. First, the advective Courant numbers, and the transported variables, are defined using primary variables u and p at appropriate temporal and spatial levels; and the advection of the variables is solved using the MPDATA algorithm. Second, the new values of pressure

are recovered from the updated pressure thicknesses, and the hydrostatic relationship provides new values of the Montgomery potential (the lower boundary condition is approximated to the second-order, using the updated values of surface pressure and s-derivatives of the pressure at the first staggered s-level). Third, having available the new values of the pressure thicknesses and Montgomery potentials, the forcing terms in the momentum equation are incorporated using the arithmetic averages from the old and new time levels; and the correction terms for the forcing-dependent truncation error term are included using the old values of the appropriate fields. Finally, the updated velocity field is recovered from the momentum variable. Such a design ensures entirely second-order approximations in the interior of the fluid. Except for the absorbing lateral and upper boundary regions, the solver employs no numerical filters or other means of explicit artificial viscosity.

The current experimental set-up assumes a uniform, undisturbed flow $U = 20\text{ms}^{-1}$, constant Brunt-Väisällä frequency $N = 2.094 \cdot 10^{-2}\text{s}^{-1}$, and the bell-shaped hill (centered at the middle of the domain),

$$h(x) = H\left(1 + \left(\frac{x}{L}\right)^2\right)^{-1} , \tag{20}$$

with a horizontal scale $L = 12 \cdot 10^3$ m and height $H = 1146$ m. The flow parameters, characteristic of a downslope windstorm regime, were selected after Miller and Durran (1991, Section 3b). The computational domain covers $22L$ and $3\lambda(\equiv 2\pi U/N)$ in the horizontal and the vertical, respectively. The regions adjacent to the lateral boundaries of width $\approx 1L$, and the upper portion of the domain of depth $\approx 1\lambda$ are designated for absorbing boundary schemes. The horizontal domain is resolved with 176 grid intervals, whereas the vertical domain is resolved with 61 isosteric levels, initially spaced at uniform 300 m intervals. The $\Delta t = 3$s time step of the computations is limited by the propagation speed of the external mode. The solutions discussed below are after 4800 time steps which is equivalent, respectively, to 24 characteristic time-scales $T(\equiv L/U)$.

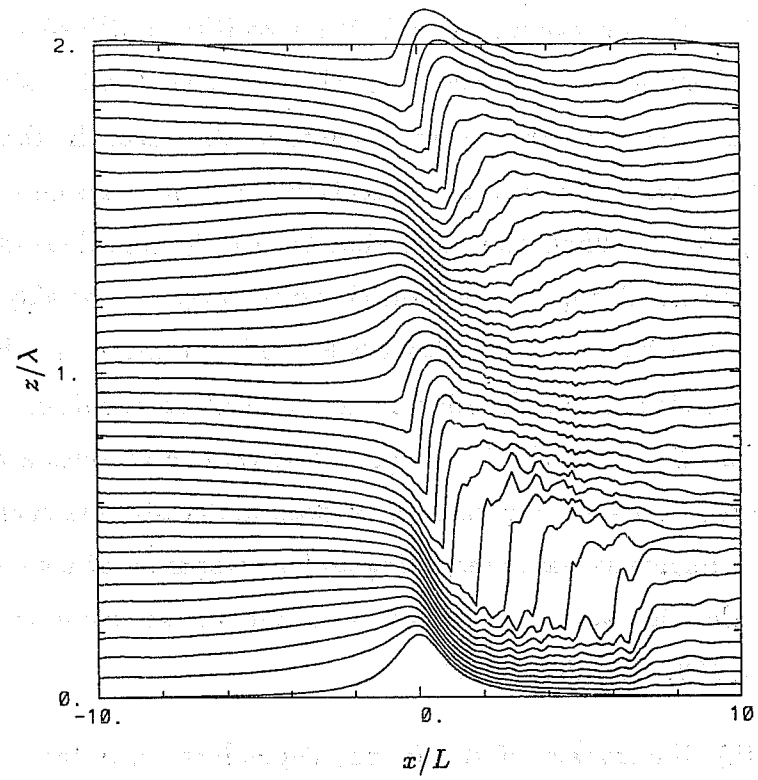

Figure 2. Constant density surfaces for calculation with the compensation of the forcing-dependent error term; this solution essentially employs no filters or other means of explicit artificial viscosity.

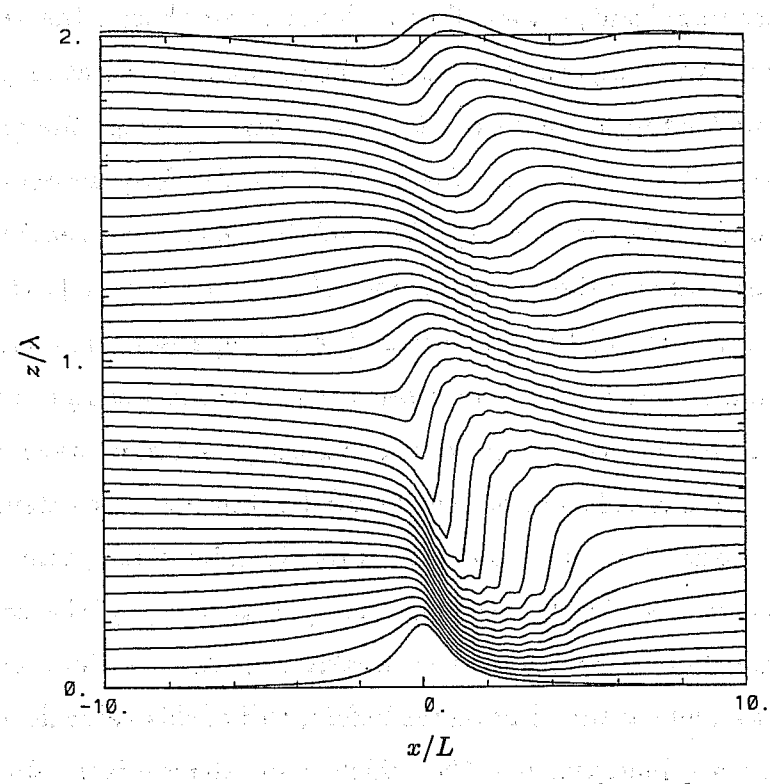

Figure 3. Constant density surfaces for calculation without the compensation of the forcing-dependent error term, but with an explicit artificial viscosity added to the momentum equation.

Figure 2 shows the solution evaluated with the algorithm outlined in the preceding paragraphs. This solution is acceptable in the sense that after short times (not shown) it compares well with the relevant solutions discussed in the literature (cf. Smolarkiewicz, 1991) and there are no indications of serious numerical problems in a long-term integration. When the correction for the forcing-dependent truncation error term in (9) is turned *off*, the solution becomes noisy and weakly unstable; as a consequence, the model "blows" soon after $t > 8T$. This solution may be stabilized by adding some weak dissipation to the r.h.s of the momentum equation. Figure 3 shows such a solution with $K = 0.02\Delta X^2/\Delta t$ (half of this value still gives a noisy solution). Although the solution is stable and smooth, it does underestimate such characteristic features of this flow regime as wave steepening and development of a neutrally-stratified region separating the high-speed shooting flow at the surface from the flow aloft (cf. Miller and Durran, 1991, for discussion).

In order to quantify the impact of the forcing-dependent error term in (11) on the overall accuracy of integrations, we compare below numerical and analytic results for a finite-amplitude flow regime, where departures from the small-amplitude linear theory solution are significant, yet small enough not to emphasize the sensitivity of the numerical solutions to the imposed boundary schemes and initialization procedure. The current experimental set-up is analogous to that in Fig. 2, except the mountain height has been reduced to $H = 477.5$ m. Figure 4 shows the fully second-order-accurate solution after $40L/U$ (8000 time-steps). This solution compares reasonably well with the analytic, steady-state solution (dashed line) of Lilly and Klemp (1979) obtained via Long's equation. The error within the domain (excluding absorbing boundary regions), measured by the maximum difference between the analytic and computational isosteres' heights, normalized by the wavelength of the standing mountain wave, is about 2.9%; the accuracy of the numerical solution may be further improved by extending the depth and width of the computational domain in order to minimize spurious influences of the boundary schemes. As in the previous example, turning *off* the compensation of the forcing-dependent error term leads to a weakly unstable solution. Adding viscosity $K = 0.02\Delta X^2/\Delta t$ stabilizes the solution (as before, half of this value does not suffice for stability); but the error increases to 4.1%, which is an intermediate value between that for the second-order solution and the 5.1% value characteristic of the first-order-solution

(not shown[7]) containing all truncation errors on the r.h.s of (11).

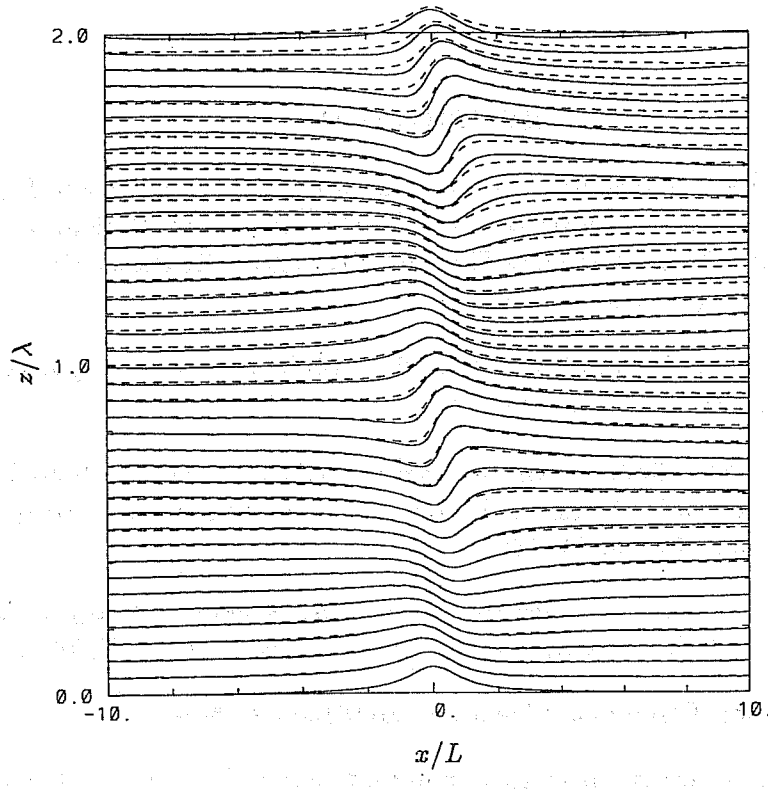

Figure 4. Steady state constant density surfaces for a small, finite-amplitude mountain. Dashed lines display the analytic solution; the solid lines are for the numerical solution with the second-order-accurate algorithm employed in Fig. 2.

4. CONCLUDING REMARKS

The examples discussed in section 3.2 clearly illustrate the practical significance of the theoretical considerations set forth in section 2. In the physical problems examined, the compensation of the first-order, forcing-dependent error term appears important as it improves not only the accuracy but also the stability of the resulting solutions. In many applications (see, for example, section 3.1), this error may be small and of no importance beyond merely degrading the formal accuracy of approximations. However, since a compensation of this error term is simple, computationally efficient, and easy to implement in any numerical model employing forward-in-time differencing,

[7] In contrast to the downslope windstorm regime (Figs. 2, and 3), differences between the three solutions discussed are relatively minor in appearance; the lower-order solutions closely resemble that in Fig. 4, except they underestimate the amplitude of the wave aloft.

it should not be neglected, especially since it is theoretically required for the dissipative approximations claiming second-order accurate solutions (section 2).

REFERENCES

Bleck, R., 1984: Linear advection. In:*Lectures presented at the workshop on limited-area numerical weather prediction models for computers of limited power*; Erice, Italy. Short- and Medium-Range Weather Prediction Research Publication Series, 8, World Met. Org., Geneva, 105–115.

——, 1984: An isentropic coordinate model suitable for lee cyclogenesis simulation. *Riv. Meteor. Aeronaut.*, **43**, 189–194.

——, and L. T. Smith, 1990: A wind-driven isopycnic coordinate model of the north and equatorial Atlantic Ocean. 1. Model development and supporting experiments. *J. Geophys. Res.*, **95C**, 3273–3285.

Bott, A., 1989: A positive definite advection scheme obtained by nonlinear renormalization of the advective fluxes. *Mon. Wea. Rev.*, **117**, 1006–1015.

Crowley, W. P., 1968: Numerical advection experiments. *Mon. Wea. Rev.*, **96**, 1–11.

Davies, H. C., 1983: Limitations of some common lateral boundary schemes in regional NWP models. *Mon. Wea. Rev.*, **111**, 1002–1012.

Dukowicz, J. K., and J. D. Ramshaw, 1979: Tensor viscosity method for convection in numerical fluid dynamics. *J. Comput. Phys.*, **32**, 71–79.

Gresho, P. M., S. T. Chan, R. L. Lee, and C. D. Upson, 1984: A modified finite element method for solving the time-dependent, incompressible Navier-Stokes equations. Part 1: Theory. *Int. J. Num. Meth. Fluids*, 4, 557–598.

Houghton, D. D., and A. Kasahara, 1968: Nonlinear shallow fluid flow over an isolated ridge. *Commun. Pure Appl. Math.*, **21**, 1-23.

Klemp, J. B., and D. K. Lilly, 1978: Numerical simulations of hydrostatic mountain waves. *J. Atmos. Sci.*, **35**, 78–107.

Leith, C. E., 1965: Numerical simulation of the Earth's atmosphere. In *Methods in Computational Physics*, Vol 4, edited by B. Alder, S. Ferenbach and M. Rotenberg, Academic Press, New York, 1965, 385 pp.

Lilly, D. K., and J. B. Klemp, 1979: The effects of terrain shape on nonlinear hydrostatic mountain waves. *J. Fluid Mech.*, **95**, 241–261.

Margolin, L. G., and P. K. Smolarkiewicz, 1989: Antidiffusive velocities for multipass donor cell advection. Lawrence Livermore National Laboratory. Report # **UCID-21866**, 44 pp.

Miller, P. P., and D. R. Durran, 1991: On the sensitivity of downslope windstorms to the asymmetry of the mountain profile. *J. Atmos. Sci.*, in press.

Petschek, A. G. and L. D. Libersky, 1975: Stability, accuracy, and improvement of Crowley advection schemes. *Mon. Wea. Rev.*, **103**, 1104–1109.

Richtmyer, R. D. and K. W. Morton, 1967: *Finite Difference Methods for Initial Value Problems*, Wiley-Interscience, New York, 405 pp.

Roache, P. J., 1972: *Computational Fluid Dynamics.* Hermosa Publishers, Albuquerque, 446 pp.

Rood, R. B., 1987: Numerical advection algorithms and their role in atmospheric transport and chemistry models. *Rev. Geophys.*, **25**, 71–100.

Smolarkiewicz, P. K., 1982: The multi-dimensional Crowley advection scheme. *Mon. Wea. Rev.*, **110**, 1968–1983.

_____, 1983: A simple positive definite advection scheme with small implicit diffusion. *Mon. Wea. Rev.*, **111**, 479–486.

_____, 1984: A fully multidimensional positive definite advection transport algorithm with small implicit diffusion. *J. Comput. Phys.*, **54**, 325–362.

_____, 1985: On the accuracy of the Crowley advection scheme. *Mon. Wea. Rev.*, **113**, 1425–1429.

_____, and T. L. Clark, 1986: The multidimensional positive definite advection transport algorithm: Further development and applications. *J. Comput. Phys.*, **67**, 396–438.

_____, and W. W. Grabowski, 1990: The multidimensional positive definite advection transport algorithm: Nonoscillatory option. *J. Comput. Phys.*, **86**, 355–375.

_____, 1991: On forward-in-time differencing for fluids. *Mon. Wea. Rev.*, in press.

Strang, G., 1968: On the construction and comparison of difference schemes. *SIAM J. Numer. Anal.*, **5**, 506–517.

Smith, R. B., 1989: Linear theory of stratified flow past an isolated mountain in isosteric coordinates. *J. Atmos. Sci.*, **45**, 3889–3896.

Takacs, L. L., 1985: A two-step scheme for the advection equation with minimized dispersion errors. *Mon. Wea. Rev.*, **113**, 1050–1065.

Tremback, C. J., J. Powell, W. R. Cotton, and R. A. Pielke, 1987: The forward-in-time upstream advection scheme: Extension to higher orders. *Mon. Wea. Rev.*, **115**, 540–555.

Warming, R. F., and B. J. Hyett, 1974: The modified equation approach to the stability and accuracy analysis of finite-difference methods. *J. Comput. Phys.*, **14**, 159–179.